

Activated dynamics at a non-disordered critical point

D. DAS, J. KONDEV and B. CHAKRABORTY

*Martin Fisher School of Physics, Brandeis University
Mailstop 057, Waltham, MA 02454-9110, USA*

(received 3 April 2002; accepted in final form 11 December 2002)

PACS. 64.70.Pf – Glass transitions.

PACS. 61.20.Lc – Time-dependent properties; relaxation.

PACS. 64.60.Cn – Order-disorder transformations; statistical mechanics of model systems.

Abstract. – We present a non-randomly, frustrated lattice model which exhibits activated dynamics at a critical point. The phase transition involves ordering of large-scale structures which occur naturally within the model. Through the construction of a coarse-grained master equation, we show that the time scales diverge exponentially while the static fluctuations exhibit the usual power law divergences. We discuss the relevance of this scenario in the context of the glass transition in supercooled liquids.

One of the most striking features of supercooled liquids approaching the glass transition is a precipitous slowing down of the dynamics with no obvious structural changes. Relaxation times are observed to grow by more than ten orders of magnitude as the temperature is decreased by less than a factor of two [1]. A natural explanation of this exponential growth, often quantified by the Vogel-Fulcher-Tammann (VFT) formula [2], is the existence of a critical point with diverging free-energy barriers. This scenario is explicitly realized in the random field Ising model [3], and a scaling theory of the glass transition has been proposed based on the existence of such a critical point [4]. However, an explicit realization of this scenario in a model with *no quenched-in disorder* has, to our knowledge, not been demonstrated. The VFT form itself has been obtained from a scaling analysis of a diffusion-deposition model [5]

Another piece of the glass puzzle, the presence of dynamical heterogeneities —large clusters of fast moving particles— was uncovered recently near the glass transition in experiments on colloids [6] and in simulations of Lennard-Jones liquids [7]. Inspired by the questions raised by recent experiments, we have investigated a non-disordered, frustrated, lattice model which exhibits activated dynamics at a critical point, and where the diverging barriers arise from extended spatial structures.

Over the years, different theories of the glass transition have highlighted different aspects of the problem. The frustration-limited domain theory [1,8] relates the activated nature of the dynamics to a critical point “avoided” due to frustration imposed by competing interactions. The random first-order transition theory [9] relies on the presence of frustration in glass formers to provide for an extensive number of metastable states, which are responsible for the dynamical behavior observed near the glass transition. A very different perspective on the glass transition is provided by the mode coupling theory which predicts a purely dynamical critical

point [10] with a diverging time scale and no diverging length scale. Kinetically constrained lattice models have been constructed based on this observation [11] and it has been argued that constraints can lead to dynamical heterogeneities [12]. These models however do not usually exhibit a finite-temperature, dynamical critical point.

Below we show that glassy dynamics can emerge, upon coarse-graining, in the vicinity of a phase transition which involves ordering of large-scale structures, such as system-spanning loops. While the static fluctuations exhibit the usual power law divergences, the processes of rearranging the extended structures lead to activated dynamics. We construct a master equation for the order parameter which makes explicit the microscopic origin of the exponentially diverging time scales at the transition.

Loop model. – In constructing a lattice model of the glass transition we focused on three key features: frustration, the presence of extended spatial structures, and the existence of a thermodynamic critical point. A model which has these attributes (as shown in detail below) is the 3-coloring model on a honeycomb lattice [13] whose configurations are different bond colorings of the lattice. Each bond is colored either A , B or C , with a constraint which forbids bonds of the same color meeting at a vertex. The number of colorings is exponential in the number of vertices leading to an extensive entropy. The entropy per site is maximized when the three bonds colors are equally distributed among the three lattice directions. A coloring where all bonds in one direction are of the same color has zero entropy per site. By introducing an energy parameter which favors colorings in this zero-entropy sector a phase transition can be induced in the model.

The bond coloring constraint gives rise to *extended structures* in the form of alternating-color loops. Since the constraint enforces that there is one A colored bond and one B colored bond at every vertex, the A and B colored bonds necessarily form loops (same holds true for color pairs AC and BC). All the properties of the model, including the correlations of the colors, can be traced back to the statistics of the ensemble of loops. These loops do not intersect and they have a definite orientation ($ABAB\dots$ vs. $BABA\dots$) and can be identified with equal height contours of a discrete *height field* which lives on the dual triangular lattice [14].

A height field $h(x, y)$ is associated with a 3-coloring by assigning a height change $\Delta = -1$ with the colors A and B , and $\Delta = +2$ with the color C and positive directions for all the bonds is defined by orienting all the up-pointing triangles clockwise. The height at the origin is fixed (to, say, zero) and increases along the positive directions by an amount Δ , each time a (colored) bond of the honeycomb lattice is crossed. (Details of the height mapping can be found in refs. [14, 15].)

The lattice that we use has $2L^2$ sites and $3L^2$ bonds with periodic boundary conditions. The three lattice directions, with relative orientation of 60° to each other, are indexed by $\alpha = 1(\equiv x), 2(\equiv y), 3$. We introduce a long-range interaction energy between the C colors, with a parameter μ measuring the strength of this interaction:

$$E = -\frac{\mu}{L^2} \sum_{\alpha=1,2,3} (2N_C^\alpha - L^2)^2. \quad (1)$$

Here N_C^α is the total number of C bonds in the α -direction. The energy is minimized if the C colors all align in one of the three directions. In the completely disordered state the energy is $E_{\max} = -\mu L^2/3$, while in the completely ordered state it is $-3\mu L^2$. As the value of the coupling constant μ is increased from 0, the system undergoes a phase transition from a disordered to an ordered phase.

The phase transition is best described in terms of the height representation of the model. In the disordered phase, where the colors are equally divided among the three lattice directions,

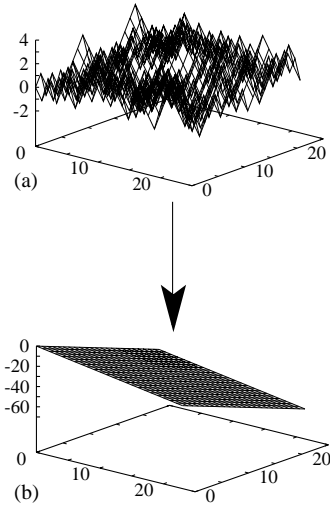


Fig. 1

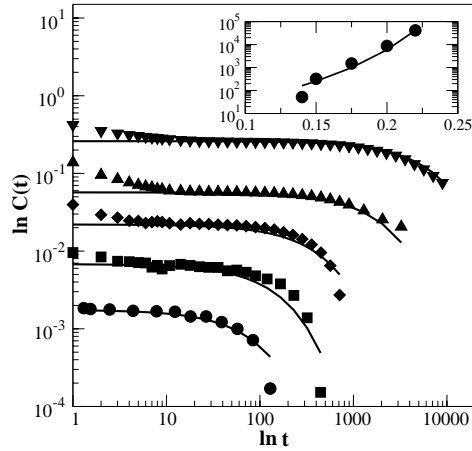


Fig. 2

Fig. 1 – Height profiles in the (a) disordered, and (b) ordered states for $L = 24$. The x - and y -axes denote the lattice coordinates, and the z -axis gives the height.

Fig. 2 – $C(t)$ (dimensionless) vs. t ($2L^2$ MCS), at $\mu = 0.14, 0.15, 0.175, 0.2$, and 0.22 (from bottom to top) for $L = 24$. The inset shows a plot of τ (obtained by setting $C(\tau) = 10^{-3}$) against μ and a VFT fit to it.

the height forms a *rough untilted* surface. Figure 1(a) shows the height in a typical disordered state. If the energy completely dominates and all the C 's align in one direction, then the surface is *smooth and tilted*, as shown in fig. 1(b). Tuning the energy coupling induces a tilting transition of the surface. The exact nature of the tilting transition in the 3-color model is not known. The following argument ensures, however, that the tilting transition in the 3-color model occurs at a finite $\mu = \mu_*$. The entropy is maximum when the surface is rough and untilted [13]. Therefore for small tilts $\boldsymbol{\rho} = (\rho_x, \rho_y)$, where $\rho_x = \langle h(L, y) - h(0, y) \rangle_y / 3$ and $\rho_y = \langle h(x, L) - h(x, 0) \rangle_x / 3$ are the tilt components (L is the linear system size), the entropy can be expressed as: $S \simeq S_{\max} - \boldsymbol{\rho} \cdot [\mathcal{S} \cdot \boldsymbol{\rho}]$. Here S_{\max} is the maximum entropy [13] and \mathcal{S} is a 2×2 positive matrix. From eq. (1) it follows that the energy is also quadratic in $\boldsymbol{\rho}$:

$$E = E_{\max} - 8\mu(\rho_x^2 + \rho_y^2 - \rho_x\rho_y). \quad (2)$$

Therefore, the free energy, $F = E - S$, which is concave at $\mu = 0$, must change its curvature at some finite μ_* , when E balances S . The exact dependence of entropy S on the tilt $\boldsymbol{\rho}$ is difficult to calculate in this model. Instead, to confirm the above scenario, we measured numerically the equilibrium probability distribution $P^{\text{eq}}(\boldsymbol{\rho})$ for different values of μ . The distribution becomes broader with increasing μ . Quadratic fits to P^{eq} , when extrapolated, indicate a transition at $\mu_* \simeq 0.4 \pm 0.05$, where the curvature of the free energy at $\boldsymbol{\rho} = 0$ vanishes. A tilting transition at a finite μ_* has been explicitly demonstrated in a closely related dimer model through an exact calculation [16] and lends further support to our argument.

Loop dynamics. – The color constraint imposes severe restrictions on the allowed paths in the configuration space of the 3-coloring model, as no local color updates are possible. To investigate the critical dynamics at the transition from the rough untilted surface to the flat tilted state, we make use of Metropolis dynamics involving alternating-color loops.

In one Monte Carlo step of our simulation, we randomly choose a site, and choose either an $A - B$, $B - C$ or a $C - A$ loop passing through it. Then we exchange the two colors along the chosen loop using ordinary Metropolis rules. Since the energy function defined in eq. (1) depends on global numbers N_C^α , it is easy to see that all local loop updates are zero energy-change moves. Only when system spanning loops with non-zero winding numbers are chosen for updating, does the possibility of a non-zero energy change arise. Therefore, the tilting of the surface and hence the lowering of energy can only be brought about by updates of system-spanning loops which introduce integer-valued changes in ρ_x or ρ_y .

Simulation results. – To characterize the dynamics of the tilting transition, we measure the equilibrium tilt-tilt autocorrelation function, which corresponds to the slowest mode in the system:

$$C(t) = \frac{\langle (\boldsymbol{\rho}(t+t_0) - \langle \boldsymbol{\rho} \rangle) \cdot (\boldsymbol{\rho}(t_0) - \langle \boldsymbol{\rho} \rangle)) \rangle}{\langle (\boldsymbol{\rho}(t_0) - \langle \boldsymbol{\rho} \rangle)^2 \rangle}. \quad (3)$$

Here $\langle \dots \rangle$ denotes an average over various initial times t_0 in a history, and over several histories. In fig. 2 we show $C(t)$ at different μ , *approaching* the tilting transition from below, for $L = 24$. The unit of time t is $2L^2$ Monte Carlo steps (MCS). Similar curves have been obtained for two other system sizes, $L = 36$ and $L = 48$. It is clear from the curves shown in fig. 2, that the relaxation time increases as μ is increased. To characterize this increase of time scales, we adopt an operational definition of the relaxation time τ via $C(\tau) = C_0$, where C_0 is an arbitrary small number; in experiments C_0 is the smallest measurable $C(t)$. Such a definition of τ was used earlier in refs. [17, 18]. As shown in the inset to fig. 2, with $C_0 = 10^{-3}$, τ grows by four orders of magnitude as μ is changed from 0.14 to 0.22. Since a critical point occurs in our model at $\mu_* \simeq 0.4$, τ is expected to diverge at this point. The growth of τ shown in fig. 2 is consistent with the VFT form, $\exp[A/(\mu_* - \mu)]$, or a power law divergence with an unusually large exponent $\simeq 14$.

Master equation for tilt. – The VFT divergence of the relaxation time is a generic feature of real glass formers and the origin of this anomalous slowing-down is still a matter of some debate. Within our simple model we investigate the crucial features underlying the rapid rise in time scales, by measuring the transition probabilities among different tilted states and constructing a coarse-grained dynamical model for the tilt relaxation. We find that the relaxation process is very different from simple Langevin dynamics within a concave free-energy well and is, instead, dominated by traps and barriers.

The system is prepared in an initial state with tilt $\boldsymbol{\rho} = (0, \rho)$ or $(\rho, 0)$ ⁽¹⁾. It stays in this tilt state for time t and makes a transition to a new state ρ' in the next time interval δt . The measurements involve collecting 10^4 – 10^5 time histories for each value of the initial tilt. From these time histories we calculate $P_{\rho \rightarrow \rho}$, the probability that the system stayed in the state ρ for time $t + \delta t = n\delta t$, and $P_{\rho \rightarrow \rho'}$, the probability that it stayed in the state ρ for time t and made a transition to ρ' between t and $t + \delta t$.

If the tilt configurations $\{\rho\}$ evolve via a Markov process, then the probabilities are exponential: $P_{\rho \rightarrow \rho} = f_1 \exp[-t/\tau_\rho]$ and $P_{\rho \rightarrow \rho'} = f_2 \exp[-t/\tau_\rho]$, where f_1 and f_2 are numbers less than unity. Our simulations confirm this for all values of μ and ρ ($\rho \neq 0$) that we studied and validates the Markovian description of the dynamics in terms of the (coarse-grained) states $\{\rho\}$. The $\rho = 0$ states are an exception since we found that $P_{0 \rightarrow 0}$ is a stretched exponential in t . This observation has no bearing on our current discussion, and will be taken up in a future paper.

⁽¹⁾Although the boundary conditions allow the system to have any tilt $\boldsymbol{\rho}$, to simplify our discussion of transition probabilities, we restrict our attention to states with a tilt pointing in the x - or y -direction only.

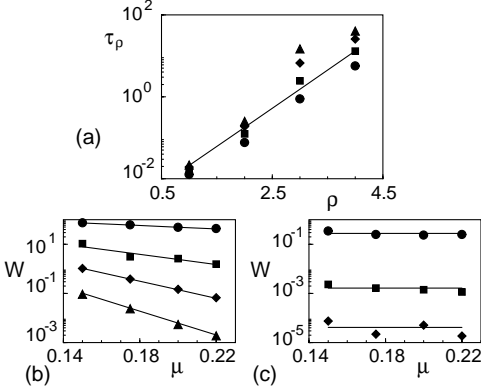


Fig. 3

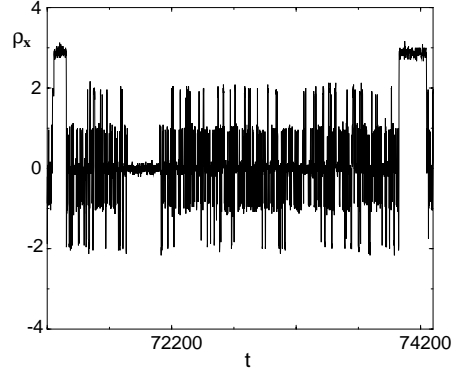


Fig. 4

Fig. 3 – (a) Relaxation times for simple tilts, τ_ρ , as a function of ρ , for $\mu = 0.15, 0.175, 0.2$ and 0.22 (from bottom to top); (b) the transition matrix elements $W_{\rho-1,\rho}$ vs. μ , for $\rho = 1, 2, 3$ and 4 (from top to bottom), and (c) $W_{\rho+1,\rho}$ vs. μ for $\rho = 1, 2$ and 3 (from top to bottom). The straight line in (a) corresponds to a simple exponential growth, while the lines in (b) and (c) are fits to eqs. (5) and (6).

Fig. 4 – Typical trace of the ρ_x component of the tilt as a function of time, measured in $2L^2$ MCS, for system size $L = 24$ and $\mu = 0.275$ (only simple tilts were allowed). The time window chosen is such that $\tau_2 \ll t \ll W_{3,2}^{-1}$, where $\tau_2 = 2$ and $W_{3,2}^{-1} = 20000$. During this time the system equilibrates among all states with $|\rho_x| \leq 2$.

Since the dynamics is Markovian, the measurements of $P_{\rho \rightarrow \rho}$ and $P_{\rho \rightarrow \rho'}$ can be used directly to calculate the relaxation times τ_ρ , and the transition matrix elements $W_{\rho' \rho}$ from ρ to ρ' :

$$\sum_{\rho' \neq \rho} W_{\rho' \rho} = \tau_\rho^{-1}, \quad W_{\rho' \rho} = \tau_\rho^{-1} \frac{f_2}{1 - f_1}. \quad (4)$$

The variation of τ_ρ with the tilt ρ is shown in fig. 3(a) for different values of μ . The most striking feature of these time scales is that τ_ρ increases dramatically with ρ . The best fit to the data leads to an exponential growth: $\tau_\rho \propto \exp[\alpha \rho^{2\gamma}]$, with γ between $1/2$ and 1 . We will show below that the exponential increase of τ_ρ is a direct consequence of the unusual form of the transition rates between different tilted states. Moreover, this exponential divergence of τ_ρ leads to a VFT-type divergence of the relaxation time τ . To explore the origin of the exponential rise of τ_ρ with ρ , we investigated the elements of the transition matrix W obtained from our measurements. The transition rates $W_{\rho-1,\rho}$, and $W_{\rho+1,\rho}$ are plotted in fig. 3(b) and (c), respectively [19].

The measurement errors for the transition rates from higher to lower tilt (fig. 3(b)) are smaller than the symbol size. These rates are well fitted by $\exp[-8\mu(2\rho - 1)]$, which means that they are of the form

$$W_{\rho-1,\rho} = \Gamma_0 e^{-(E_{\rho-1} - E_\rho)}. \quad (5)$$

The μ -independent factor Γ_0 varies rather weakly (about a factor of 2 for the data in fig. 3(b)) with ρ . Therefore, the relaxation of ρ to $(\rho - 1)$ is dominated by the cost of going uphill in energy. In what follows, we assume that eq. (5) continues to hold close to the critical point. This predicts specific forms for the μ - and ρ -dependence of $W_{\rho+1,\rho}$ and τ_ρ , which are both confirmed by our numerics.

From detailed balance, which we have explicitly checked for all μ 's using the measured $P^{\text{eq}}(\rho)$ and $W_{\rho',\rho}$, we conclude that the transitions from ρ to $(\rho + 1)$ are controlled by the change in entropy between the two tilt states. Therefore the appropriate transition matrix elements can be written as

$$W_{\rho+1,\rho} = \Gamma_0 e^{S_{\rho+1} - S_\rho} \equiv \Gamma_0 \Gamma(\rho), \quad (6)$$

with a $\Gamma(\rho)$ independent of μ and exponentially dependent on ρ . As seen in fig. 3(c), this is confirmed by direct measurements of $W_{\rho+1,\rho}$. Combining eqs. (4), (5), and (6) leads to

$$\tau_\rho = \frac{1}{W_{\rho+1,\rho} + W_{\rho-1,\rho}} = \frac{1/\Gamma_0}{\Gamma(\rho) + e^{-(E_{\rho-1} - E_\rho)}}. \quad (7)$$

The dramatic suppression of the downhill transitions, reflected in $\Gamma(\rho) \ll \exp[-(E_{\rho-1} - E_\rho)] < 1$ (cf. fig. 3(c)), leads to a τ_ρ dominated by the exponential energy cost of decreasing the tilt. This is borne out by the numerics presented in fig. 3(a).

The partitioning of the rates into one which depends purely on the energy change and another which depends purely on the entropy change is in sharp contrast to the usual symmetric partitioning where both depend on free-energy differences. The microscopic origin of the rate asymmetry can be argued to follow from the spatial blocking caused by the system spanning loops in a tilted state. These loops are meandering objects with lengths that scale as $L^{3/2}$ [15, 20]. Thus, in order to increase the tilt, entropic repulsion between the loops must be overcome. Transitions to higher tilt states are therefore controlled by the entropy loss when increasing ρ (cf. eq. (6)). An asymmetry of rates similar to what we find was postulated in the tiling model for glasses [21], and was shown to lead to slow dynamics.

Theory of Vogel-Fulcher-Tammann divergence. – Starting from eq. (3) for the correlation function, we can write

$$C(t) = \frac{\sum_\rho \rho^2 P_1(\rho, t | \rho, 0) P_{\text{eq}}(\rho)}{\sum_\rho \rho^2 P_{\text{eq}}(\rho)} + \frac{\sum_{\rho \neq \rho'} \rho \rho' P_1(\rho, t | \rho', 0) P_{\text{eq}}(\rho')}{\sum_\rho \rho^2 P_{\text{eq}}(\rho)}. \quad (8)$$

In the above equation, P_1 is the conditional probability that at time t the tilt is ρ given that at time 0 it was ρ' . We measured $P_1(\rho, t | \rho, 0)$ and found that it is well approximated by $\exp[-t/\tau_\rho]$. Furthermore, for $t < \tau_\rho$, the off-diagonal probability $P_1(\rho, t | \rho', 0)$ is negligible compared to the diagonal one, while for $t > \tau_\rho$, $P_1(-\rho, t | \rho', 0) = P_1(\rho, t | \rho', 0)$. We conclude that the second term in eq. (8) does not contribute, and to a very good approximation:

$$C(t) \approx \frac{\sum_\rho \rho^2 e^{-t/\tau_\rho} P_{\text{eq}}(\rho)}{\sum_\rho \rho^2 P_{\text{eq}}(\rho)}. \quad (9)$$

To check this formula we calculated the right-hand side using the measured P_{eq} and τ_ρ , and compared it to the measured $C(t)$; we found good agreement. The reason for the simple form of $C(t)$ is the exponential separation of time scales over which the system explores ever-increasing tilts. For example, during a time t such that $\tau_\rho \ll t \ll W_{\rho+1,\rho}^{-1}$ the system equilibrates completely among states with tilts whose magnitude is $\leq |\rho|$ (see fig. 4). States with tilts greater than $|\rho|$ are only accessed beyond time $W_{\rho+1,\rho}^{-1}$. The form of the autocorrelation function (eq. (9)), which emerges naturally from the microscopic lattice model upon coarse-graining, is similar to that of the trap model of glasses [18].

Substituting the observed forms, $\tau_\rho \sim \exp[\alpha\rho^{2\gamma}]$, and $P_{\text{eq}}(\rho) \sim \exp[-|\mu - \mu_*|\rho^2]$ in eq. (9), and performing a saddle point analysis for large t leads to $C(t) \sim C_1 \exp[-|\mu - \mu_*|(\frac{1}{\alpha} \ln |\frac{\alpha\gamma t}{|\mu - \mu_*|})^{\frac{1}{\gamma}}]$. For $\gamma = 1$, $C(t)$ follows a simple power law: $C(t) \sim t^{-|\mu - \mu_*|/\alpha}$. For $\gamma < 1$, the decay of $C(t)$ is faster than a power law but slower than a stretched exponential. For general values of γ , the relaxation time τ defined by $C(\tau) = C_0$, diverges according to the VFT form:

$$\tau \sim \exp \left[\alpha \left(\ln \frac{C_1}{C_0} \right)^\gamma \left(\frac{1}{|\mu - \mu_*|} \right)^\gamma \right]. \quad (10)$$

The μ -dependence of τ obtained from the saddle point analysis is consistent with the data shown in fig. 2, even though the predicted asymptotic limit, characterized by a power law decay of $C(t)$, was not achieved in our simulations.

Conclusion. – In summary, we find that a lattice model with frustration and associated extended structures exhibits trap-dominated, activated dynamics near a critical point. The phase transition involves rearrangements of these structures which leads to *jamming* and exponentially diverging time scales. The model suggests that focusing on the effective dynamics of extended structures in atomistic simulations of glasses, and experiments, might yield new insight into the cause of the dramatic slowing down of relaxations as the glass transition is approached.

* * *

We thank J. P. SETHNA, S. KIVELSON, R. STINCHCOMBE, M. BARMA, D. DHAR and G. TARJUS for helpful discussions. This work was supported by the NSF DMR-9815986 (DD, BC) and NSF DMR-9984471 (JK).

REFERENCES

- [1] TARJUS G., KIVELSON D. and VIOT P., *J. Phys. Condens. Matter*, **12** (2000) 6497.
- [2] VOGEL H., *Phys. Z.*, **22** (1921) 645; FULCHER G. S., *J. Am. Ceram. Soc.*, **8** (1925) 339.
- [3] FISHER D. S., *Phys. Rev. Lett.*, **56** (1986) 416.
- [4] SETHNA J. P., SHORE J. D. and HUANG M., *Phys. Rev. B*, **44** (1991) 4943.
- [5] STINCHCOMBE R. and DEPKEN M., *Phys. Rev. Lett.*, **88** (2002) 125701.
- [6] WEEKS E. R., CROCKER J. C., LEVITT A. C., SCHOFIELD A. and WEITZ D. A., *Science*, **287** (2000) 627.
- [7] DONATI C. *et al.*, *Phys. Rev. E*, **60** (1999) 3107, and references therein.
- [8] KIVELSON S. A. *et al.*, *J. Chem. Phys.*, **101** (1994) 2391.
- [9] WESTFAHL H. jr. *et al.*, *Phys. Rev. B*, **64** (2001) 174203.
- [10] GÖTZE W. and SJÖGREN L., *Rep. Prog. Phys. B*, **55** (1992) 241.
- [11] JÄCKLE J. and EIZINGER S., *Z. Phys. B*, **84** (1991) 115.
- [12] GARRAHAN J. P. and CHANDLER D., cond-mat/0202392 Preprint, 2002.
- [13] BAXTER R. J., *J. Math. Phys.*, **11** (1970) 784.
- [14] KONDEV J., DEGIER J. and NIENHUIS B., *J. Phys. A*, **29** (1996) 6489.
- [15] CHAKRABORTY B., DAS D. and KONDEV J., *Eur. Phys. J. E*, **9** (2002) 227.
- [16] YIN H. and CHAKRABORTY B., *Phys. Rev. Lett.*, **86** (2001) 2058.
- [17] GROUSSON M., TARJUS G. and VIOT P., cond-mat/0111305 Preprint, 2001.
- [18] MONTHUS C. and BOUCHAUD J.-P., *J. Phys. A*, **29** (1996) 3847.
- [19] Transition matrix elements only depend on the magnitude of the tilt.
- [20] KONDEV J. and HENLEY C. L., *Phys. Rev. Lett.*, **74** (1995) 4580.
- [21] WEBER T. W., FREDRICKSON G. H. and STILLINGER F. H., *Phys. Rev. B*, **34** (1986) 7641.